Signal Processing 113 (2015) 61–67

Contents lists available at ScienceDirect

Signal Processing

journal homepage: www.elsevier.com/locate/sigpro

Fast communication

# Design of high-order rotation invariants from Gaussian–Hermite moments

Bo Yang [a,b], Jan Flusser [a,*], Tomáš Suk [a]

[a] Institute of Information Theory and Automation of the CAS, Pod Vodárenskou věží 4, 18 208 Prague 8, Czech Republic
[b] School of Automation, Northwestern Polytechnical University, 127 West Youyi Road, 710 072 Xi'an Shaanxi, P.R. China

ARTICLE INFO

*Article history:*
Received 5 August 2014
Received in revised form
14 December 2014
Accepted 5 January 2015
Available online 30 January 2015

*Keywords:*
Rotation invariants
Geometric moments
Gaussian–Hermite moments
Recurrent relation

ABSTRACT

In this paper we proposed a method to design and numerically calculate high-order rotation invariants from Gaussian–Hermite moments. We employed the invariant properties of the Gaussian–Hermite moments discovered earlier in [1] and we showed how to construct rotation Gaussian–Hermite invariants even in the cases when no explicit invariants from geometric moments are available. We verify by experiments the rotation invariance and show that we are capable of computing much higher order of Gaussian–Hermite invariants than of geometric invariants, which brings better discrimination power.



## 1. Introduction

Rotation invariants play a key role in position-invariant object description and recognition. Being a part of rigid-body transformation, object rotation is present almost in all applications, even if the imaging system is well set up and the experiment has been prepared in a laboratory. On the other hand, rotation is not trivial to handle mathematically, unlike for instance translation and scaling. For these two reasons, invariants to rotation have been in focus of researchers since the beginning. Invariants composed of image moments, *moment invariants*, belong to the most popular ones [2].

Moment invariants have been mostly constructed from *geometric moments*, which are projections of an image onto a standard polynomial basis $x^p y^q$ [3]. Several authors realized the limitations of geometric moments, namely their numerical instability, and proposed to employ various orthogonal moments instead. Teague [4], Khotanzad and Hong [5], and Wallin and Kübler [6] used Zernike moments, the other authors employed Legendre [7], Krawtchouk [8], and Fourier–Mellin [9] moments. Most recently, Yang and Dai [1] have proposed invariants from Gaussian–Hermite moments.

Gaussian–Hermite invariants (GHIs) combine two favorable properties. From theoretical point of view, their construction is straightforward. Yang and Dai proved that any function of geometric moments which is invariant to rotation keeps the invariance if geometric moments are replaced by Gaussian–Hermite moments. This is the central theorem of [10] showing that the GHIs, unlike the other invariants from orthogonal moments, can be obtained directly as soon as the geometric moment invariants have been derived. From computational point of view, the Gaussian–Hermite moments are similar to the other orthogonal moments, more stable and robust to numerical errors than the geometric moments. This is because the orthogonal polynomials can be evaluated by recurrent relations which allows computation with higher precision than the direct algorithms. These two properties – easy derivation

* Corresponding author
*E-mail addresses:* bo.yang@hotmail.fr (B. Yang), flusser@utia.cas.cz (J. Flusser), suk@utia.cas.cz (T. Suk).

http://dx.doi.org/10.1016/j.sigpro.2015.01.005
0165-1684/

and stable computation – make the GHIs powerful object descriptors, as was proved in [1,10].

The only weak link of the above consideration is that rotation invariants from geometric moments have been explicitly derived up to the order five only in the literature. The goal of this paper is to bridge this gap and to show how to derive and calculate higher-order GHIs. In this sense this paper is an extension of the recent paper [1] published in this journal.

## 2. Gaussian–Hermite moments

Gaussian–Hermite moments (GHMs) were exhaustively described in [1,10]. Here we recall basic formulae which are needed for derivation of the invariants.

Hermite polynomials are defined as

$$H_p(x) = (-1)^p \exp(x^2) \frac{d^p}{dx^p} \exp(-x^2). \tag{1}$$

They are orthogonal on $(-\infty,\infty)$ with a Gaussian weight function:

$$\int_{-\infty}^{\infty} H_p(x) H_q(x) \exp(-x^2) dx = 2^p p! \sqrt{\pi} \delta_{pq} \tag{2}$$

and they can be efficiently computed by the following three-term recurrence relation:

$$H_{p+1}(x) = 2xH_p(x) - 2pH_{p-1}(x) \quad \text{for } p \geq 1, \tag{3}$$

with the initial conditions being $H_0(x) = 1$ and $H_1(x) = 2x$.

For the definition of Gaussian–Hermite moments, we move the coordinate origin to the image centroid, scale Hermite polynomials by a parameter $\sigma$ and modulate them by a Gaussian function with the same parameter. Hence, the (centralized) Gaussian–Hermite[1] moment $\overline{\eta}_{pq}$ of order $(p+q)$ of function $f(x,y)$ is defined as

$$\overline{\eta}_{pq} = \int_{-\infty}^{\infty} \int_{-\infty}^{\infty} H_p\left(\frac{x}{\sigma}\right) H_q\left(\frac{y}{\sigma}\right) \exp\left(-\frac{x^2+y^2}{2\sigma^2}\right) f(x,y)\, dx\, dy. \tag{4}$$

Recalling the geometric moments (GMs)

$$m_{pq} = \int_{-\infty}^{\infty} \int_{-\infty}^{\infty} x^p y^q f(x,y)\, dx\, dy \tag{5}$$

we can summarize the most important invariant property of the GHMs as follows: given a functional $I(f, m_{pq})$, $p,q = 0,1,\ldots,r$ which is invariant under an in-plane rotation of $f$, then functional $I(f, \overline{\eta}_{pq})$ is also an invariant (see [10] for the proof).

## 3. Constructing Gaussian–Hermite invariants

### 3.1. Definition of the invariants

The main obstacle preventing us from deriving Gaussian–Hermite invariants (GHIs) of higher orders is that rotation invariants $I(f, m_{pq})$ from geometric moments have been derived explicitly up to the order five only. These low-order invariants may be sufficient in simple tasks but do not provide enough discrimination power if the object classes are similar.

To derive higher-order GHIs, we adopt the trick which was originally proposed by Flusser [3] to construct higher-order geometric invariants. Geometric moments (5) are transformed under image rotation in a relatively complicated way. Hence, Flusser [3] proposed not to work with individual geometric moments but rather with certain linear combinations[2] of the moments of the same orders:

$$c_{pq} = \sum_{k=0}^{p} \sum_{j=0}^{q} \binom{p}{k} \binom{q}{j} (-1)^{q-j} i^{p+q-k-j} m_{k+j,p+q-k-j}, \tag{6}$$

where $i$ is the imaginary unit. Unlike plain geometric moments, these combinations change under rotation in a simple way as

$$c'_{pq} = c_{pq} \cdot \exp(-i(p-q)\alpha), \tag{7}$$

where $\alpha$ denotes the coordinate rotation angle. The geometric rotation invariants are then constructed easily as such products of various $c_{pq}$'s and their powers which vanish the rotation angle (see [3] for the details).

Now we construct similar formula from the GHMs:

$$d_{pq} = \sum_{k=0}^{p} \sum_{j=0}^{q} \binom{p}{k} \binom{q}{j} (-1)^{q-j} i^{p+q-k-j} \overline{\eta}_{k+j,p+q-k-j}. \tag{8}$$

As we know from [10], $d_{pq}$ must change under rotation in the same way as $c_{pq}$. Hence,

$$d'_{pq} = d_{pq} \cdot \exp(-i(p-q)\alpha). \tag{9}$$

Thanks to that, any product of the form

$$\prod_{i=1}^{n} d_{p_i q_i}^{k_i}, \tag{10}$$

where $k_i$, $p_i$, and $q_i$ $(i = 1,\ldots,n)$ are non-negative integers such that

$$\sum_{i=1}^{n} k_i (p_i - q_i) = 0, \tag{11}$$

cancels the phase shift and provides the invariance to rotation.

There are infinitely many invariants of the form (9). An independent and complete system of the GHIs of arbitrary order can be obtained as

$$\Psi(p,q) \equiv d_{pq} d_{q_0 p_0}^{p-q} \quad \text{with } p \geq q, p_0 - q_0 = 1 \tag{12}$$

where $p_0$ and $q_0$ are fixed user-defined indices such that $d_{p_0 q_0} \neq 0$ on the dataset we work with. For the sake of numerical stability it is recommended to choose them small. In the experiments in this paper, we use the simplest choice $p_0 = 2, q_0 = 1$. The constraint $p \geq q$ is imposed to avoid redundancy because

$$d_{pq} = d_{qp}^*, \tag{13}$$

where "$*$" denotes complex conjugation. The constraint $p_0 - q_0 = 1$ is not necessary, we imposed it for simplicity

[1] This moment is sometimes called non-coefficient Gaussian–Hermite moment.

[2] These combinations are called complex moments.

only. If $p_0-q_0=s$, $s>1$, then the exponent on the right-hand side of Eq. (12) would be $(p-q)/s$. Setting $s=1$ prevents the necessity of working with the roots.

An important property of the invariants (12) is that they are mutually independent and form a complete system (basis) for arbitrary order $r$. None of the elements of the basis can be expressed as a function of the other elements and any rotation invariant can be expressed by means of the basis elements only. The knowledge of the basis is a crucial point in all pattern recognition tasks because the basis provides the same discriminative power as the set of all invariants and thus minimizes the computational cost. Seemingly, one could simply use the magnitudes $|d_{pq}|$ instead of the invariants (12). The magnitudes are also rotation invariants but do not form a complete system.

### 3.2. Independence and completeness

Instead of complete formal proofs we rather provide the readers with an insight that Eq. (12) actually forms the basis. The independence is "almost" evident from the mutual independence of the GHMs, which is self-evident from the independence of the Hermite polynomials. The only question remaining is whether or not

$$\Psi(p_0,q_0)\equiv d_{p_0,q_0}d_{q_0p_0}=|d_{p_0,q_0}|^2,$$

is independent of the others. If this was not true, there would exist such invariants (different from $\Psi(p_0,q_0)$) that

$$\Psi(p_0,q_0)=\frac{\prod_{i=1}^{n_1}\Psi(p_i,q_i)^{k_i}\cdot\prod_{i=n_1+1}^{n}\Psi^*(p_i,q_i)^{k_i}}{\prod_{i=1}^{m_1}\Psi(s_i,t_i)^{\ell_i}\cdot\prod_{i=m_1+1}^{m}\Psi^*(s_i,t_i)^{\ell_i}}. \tag{14}$$

Substituting into (14) and grouping the factors $d_{p_0q_0}$ and $d_{q_0p_0}$ together, we get

$$\Psi(p_0,q_0)=\frac{d_{q_0p_0}^{\sum_{i=1}^{n_1}k_i(p_i-q_i)}\cdot d_{p_0q_0}^{\sum_{i=n_1+1}^{n}k_i(q_i-p_i)}\cdot\prod_{i=1}^{n_1}d_{p_iq_i}^{k_i}\cdot\prod_{i=n_1+1}^{n}d_{q_ip_i}^{k_i}}{d_{q_0p_0}^{\sum_{i=1}^{m_1}\ell_i(s_i-t_i)}\cdot d_{p_0q_0}^{\sum_{i=m_1+1}^{m}\ell_i(t_i-s_i)}\cdot\prod_{i=1}^{m_1}d_{s_it_i}^{\ell_i}\cdot\prod_{i=m_1+1}^{m}d_{t_is_i}^{\ell_i}}. \tag{15}$$

On the right-hand side of Eq. (15), all $d_{pq}$'s other than $d_{p_0q_0}$ and $d_{q_0p_0}$ must be cancelled and the powers of both $d_{p_0q_0}$ and $d_{q_0p_0}$ must equal one. These constraints cannot be fulfilled at the same time, which is a contradiction with the assumption.

To prove the completeness, it is sufficient to show that all $d_{pq}$'s (and, consequently, all GHMs) up to the order $r$ can be recovered from the invariants (12). This inverse problem is equivalent to solving a simple nonlinear system of equations:

$$\Psi(p,q)=d_{pq}d_{q_0p_0}^{p-q}$$

for the $d_{pq}$'s. Since the $\Psi(p,q)$'s are rotation invariants, they do not reflect the orientation of the object. Thus, there is one degree of freedom when recovering the object moments that corresponds to the choice of the object orientation. Without loss of generality, we can choose such orientation in which $d_{p_0q_0}$ is real and positive (such orientation always exists even if it may not be unique). Then we immediately obtain

$$d_{p_0q_0}=\sqrt{\Psi(p_0,q_0)}$$

and

$$d_{pq}=\Psi(p,q)d_{q_0p_0}^{q-p}$$

for any $p$ and $q$.

### 3.3. Vanishing invariants

An interesting property of the invariants (12) is that they are identically zero on certain types of objects. As we will demonstrate, this is implied by the object symmetry. Knowing vanishing (trivial) invariants is very important in practice. Often we recognize man-made objects or natural shapes which typically exhibit certain type of symmetry. The invariants, which are identically zero, do not contribute to the recognition power, increase the computational time and may even decrease the performance of the system.

Let us first discuss the so-called *N-fold rotation symmetry*, which is the most frequent symmetry type we meet in practice. An object is said to have this symmetry if it repeats itself when it rotates around its centroid by $2\pi j/N$ for all $j=1,\ldots,N$. We use this term also for $N=\infty$ where it means the circular symmetry. The object symmetry influences the values of $d_{pq}$'s in the following way: if $(p-q)/N$ is not an integer, then $d_{pq}=0$. To see this, we should recall that after rotation by $2\pi/N$ the object turns into itself and hence

$$d'_{pq}=d_{pq}\cdot\exp(-2\pi i(p-q)/N)=d_{pq},$$

which is possible only if $(p-q)/N$ is an integer or $d_{pq}=0$. In case of circular symmetry, this means that only $d_{pp}$'s can be non-zero.

In addition to the rotation symmetry, axial symmetry also contributes to vanishing of some invariants, too. Let us investigate the behavior of the invariants (12) under a reflection across an arbitrary line. Due to the rotation and shift invariance, we can limit ourselves to the reflection across the $x$-axis. Let $\overline{f}(x,y)$ be a mirrored version of $f(x,y)$, i.e. $\overline{f}(x,y)=f(x,-y)$. Clearly,

$$\overline{d_{pq}}=d_{qp}=d_{pq}^*.$$

Thus, it holds for any basic invariant $\Psi(p,q)$

$$\overline{\Psi(p,q)}=\overline{d_{pq}d_{q_0p_0}^{p-q}}=d_{pq}^*\cdot\left(d_{q_0p_0}^*\right)^{p-q}=\Psi^*(p,q).$$

This proves that the real part of any basic invariant stays constant under reflection while the imaginary part changes its sign. Now, if the object is axially symmetric, then under reflection across this axis it turns to itself, so the imaginary part of any $\Psi(p,q)$ vanishes for axially symmetric objects.

## 4. Numerical experiments

In this section, we first experimentally verify the invariance property of (12) both with respect to computer-generated and real rotations. Then, in the main experiment of the paper, we show that the use of the

GHM's instead of the geometric moments yields the possibility of working with moments of higher orders and in that way increases the discrimination power.

### 4.1. Verification of the invariance property

We used the well-known Lena image of the size 256 × 256 pixels and its seven rotated versions as the test set. Our feature vector consisted of six invariants:

$$\mathbf{W} = \left[d_{66},\ d_{67}d_{76},\ \mathrm{Re}(d_{76}d_{12}),\ \mathrm{Re}(d_{87}d_{12}),\ d_{11,11},\ \mathrm{Re}(d_{13,12}d_{12})\right]. \tag{16}$$

Due to the focus on high-order invariants we intentionally selected the invariants of orders between 12 and 15. Fig. 1 shows the values of the invariants (scaled into the range $(-10, 10)$). It can be seen that the variance of the invariants is negligible. Actually, the Mean Relative Error (MRE) of the individual invariants is 0.17%, 0.28%, 0.36%, 1.38%, 0.10%, and 0.34%, respectively, which demonstrates a perfect invariance on artificial data.

We carried out a similar experiment on the images where the rotation was introduced physically. We scanned a cartoon card "Bumblebee" in six different orientations (see Fig. 2). The resolution was 1000 × 1000 pixels. Since the scanner was not perfect, the images differ from each other slightly by illumination and we also encounter some errors at the card border. We computed the same invariants as before and plotted them in Fig. 3. We can observe some noticeable variances there but still the corresponding MREs are reasonably low: 2.14%, 3.48%, 7.71%, 5.11%, 2.96%, and 7.56%. These results demonstrate that the invariance is slightly violated because of the differences between the images but this violation is comparable to that of other moments and should not significantly affect the performance in real applications.

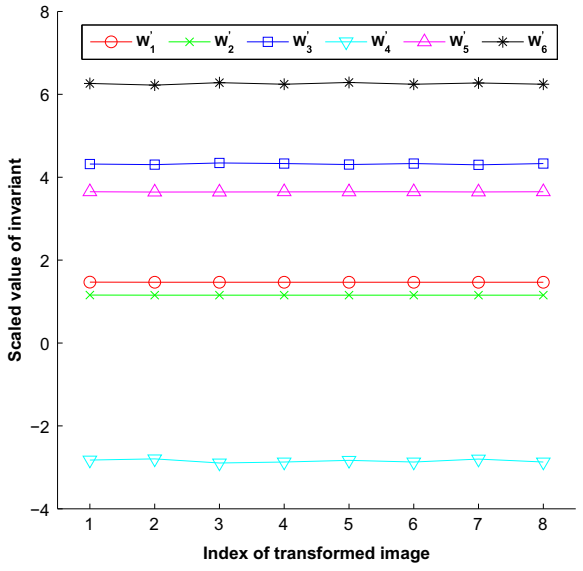


**Fig. 1.** The values of the selected invariants of rotated "Lena" images.

### 4.2. The maximum achievable order

The main reason why we prefer to use orthogonal moments is their better numerical performance compared to geometric moments. For all orthogonal moments, including Gaussian–Hermite ones, their basis functions oscillate in a reasonable range of values and can be efficiently evaluated by recurrent relations while the basis functions of geometric moments are monotonically increasing to infinity. Obviously, the computation of geometric moments brings a huge risk of numerical overflow and high order invariants from geometric moments would be unavailable in practice. In this experiment we show that the maximum achievable order (MAO) of the GHMs is much higher than that of the GMs. In the next subsection we demonstrate how the MAO influences the recognitive power of the moments.

We used 6 images shown in Fig. 4, each of them in four different resolutions: 128 × 128, 256 × 256, 512 × 512, and 1024 × 1024 pixels. For each image we tried to calculate GMs $m_{p0}$ and GHMs $\overline{\eta}_{p0}$ for $p = 0, 1, \ldots$. As $p$ increases, the values of both GMs and GHMs increase as well. Since the maximum floating-point number in standard Matlab arithmetic is $1.7977 \times 10^{308}$, one may expect that both moments overflow for certain $p > p_{max}$. This $p_{max}$ determines the maximum achievable order of the moments. Table 1 shows this $p_{max}$ for all test images.

The main results of this experiment can be summarized as follows:

- The maximum achievable order of the GHMs is always much higher than that of the GMs.
- The maximum achievable order of the GHMs is almost independent of the image size (thanks to the computation by recurrent relations) while the maximum achievable order of the GMs decreases as the image size increases.
- The maximum achievable orders of both moments do not depend much on the image content, so the results from Table 1 can be generalized to other images.

Hence, we could expect the better performance of GHIs in object recognition and retrieval, particularly in case of large images with many details where high-order invariants are required.

The MAO is a simply-to-measure criterion which only shows when the exponent overflows and which depends on the particular implementation. Another factor which also seriously influences the accuracy of the moment values is a precision loss in the mantissa. As the moment values increases and the moment order approaches the MAO, this kind of error increases, too. Due to the shape of the basis functions, GMs are much more prone to this precision loss than the GHMs, as will be demonstrated in the next subsection. Seemingly, we could avoid the overflow of GMs as long as we normalize the $(x,y)$ coordinates of the image to a square $(0, 1) \times (0, 1)$ or to another small area. This is true but the normalization brings the opposite problem. On $(0, 1)$, the monomials $x^p$ converge to zero as the power increases. When working with higher-order

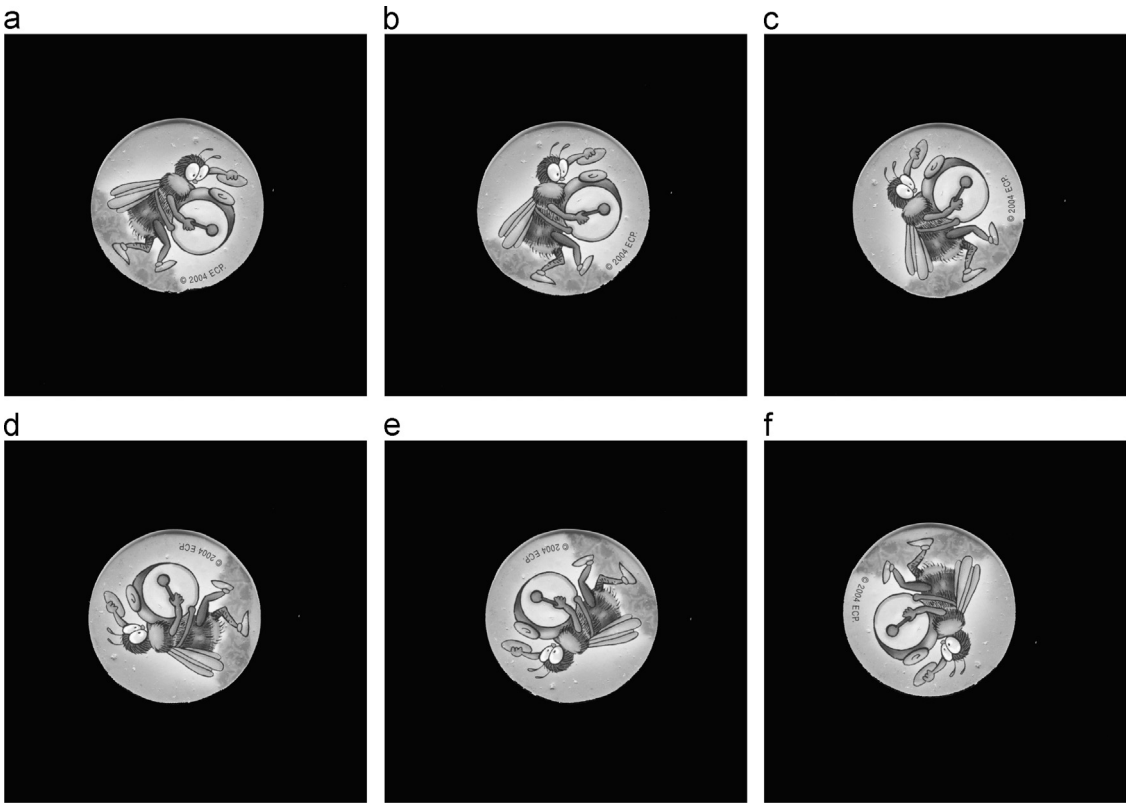


**Fig. 2.** The scanned cards "Bumblebee" whose sizes are 1000 × 1000 pixels.

moments, we face numerical "underflow" which also leads to the loss of precision. So, the normalization cannot avoid the precision loss of the GMs in principle.

### 4.3. A comparison of the recognition power

To illustrate what kind of information is contained in the higher orders and to demonstrate how the higher-order moments influence the recognition power, we performed the following experiment. The most transparent answer to the above questions is provided by studying the reconstruction abilities. The question now is – given a set of invariants up to certain order $r$, what image can be reconstructed from them and what is its difference from the original? This is equivalent to the recognition power. The reconstructed image is a representative of the equivalence class which contains, among others, also the original. Using an incomplete set of invariants, the reconstructed image cannot be equal to the original but should be close to it in some objective or subjective sense. The higher the "distance" between the reconstruction and the original, the broader this equivalence class and, consequently, the lesser the discrimination power (note that the images of the same equivalence class cannot be distinguished by the given set of the invariants).

We took the 1024 × 1024 "Cameraman" image from Fig. 4 and calculated all GM's and GHM's which can be calculated without overflow, which means up to the order 110 for GM's and 264 for GHM's (see Table 1). The difference between the invariants and the moments is irrelevant here since we are going to reconstruct the image in the fixed orientation. Thanks to Eq. (12), it does not matter whether we reconstruct from the moments or from their invariants. So, it is possible to work directly with moments.

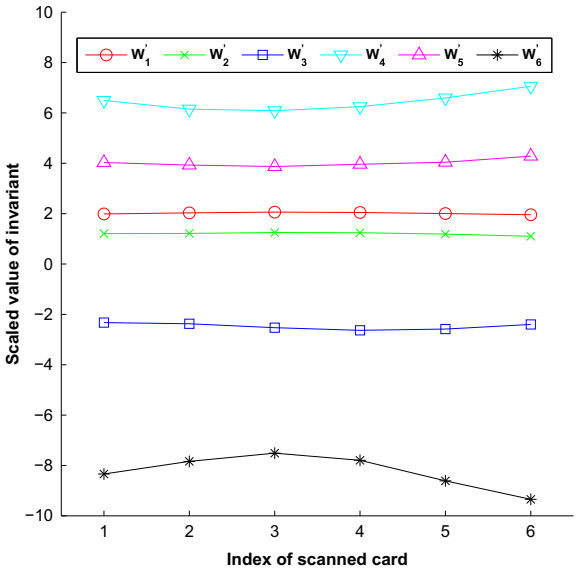


**Fig. 3.** The values of the selected invariants computed from the "Bumblebee" images.


**Fig. 4.** The test images. (a) Cameraman; (b) Baboon; (c) Barbara; (d) Lena; (e) Peppers; (f) Goldhill.

**Table 1**
The maximum achievable order $p_{max}$ computed for various images.

| Size | Cameraman | | Baboon | | Barbara | | Lena | | Peppers | | Goldhill | |
|---|---|---|---|---|---|---|---|---|---|---|---|---|
| | GM | GHM | GM | GHM | GM | GHM | GM | GHM | GM | GHM | GM | GHM |
| 128 | 165 | 265 | 168 | 265 | 167 | 265 | 167 | 265 | 168 | 265 | 166 | 265 |
| 256 | 142 | 265 | 144 | 265 | 143 | 265 | 143 | 265 | 143 | 265 | 142 | 265 |
| 512 | 124 | 264 | 125 | 264 | 125 | 265 | 125 | 264 | 125 | 264 | 124 | 264 |
| 1024 | 110 | 264 | 111 | 264 | 111 | 265 | 111 | 264 | 111 | 264 | 110 | 264 |

For the reconstruction from the GMs we used the traditional algorithm via Fourier transform, using the fact that GMs are Taylor coefficients of the image spectrum (see [2], p. 201). We used all moment up to the MAO but higher order moments are so much affected by the precision loss that they made the reconstruction completely meaningless; the reconstructed "image" is almost a random matrix with the values in the range ($-10\,000$, $10\,000$). To eliminate this effect, a standard way is to suppress high frequencies by a proper low-pass filter (see again [2], p. 201). It is unfortunately impossible to achieve a reconstruction which is close to the original. The low-pass filter smoothens the image details but if we increase the cut-off frequency the reconstructed image starts to oscillate unpredictably. The best reconstruction we were able to achieve is shown in Fig. 5. One can observe certain basic features of the original but all details are missing.

The reconstruction from the GHMs was performed directly in the image space, without employing the spectral domain, which is possible for all orthogonal moments (see [2], Section 6.5.3). Since the precision loss in mantissa is much smaller than in case of the GMs and since there are higher-order moments available, the reconstruction is much better, see Fig. 6. One can still observe some small oscillations but all important details are apparent. Note that theoretically the moments up to the order 1024 are necessary for a perfect reconstruction.

## 5. Conclusion

In this paper we proposed a method to design and numerically calculate high-order rotation invariants from Gaussian–Hermite moments. We employed the invariant properties of the Gaussian–Hermite moments discovered

**Fig. 5.** The reconstructed image "Cameraman" from GMs using moments up to order 110.

**Fig. 6.** The reconstructed image "Cameraman" from GHMs using moments up to order 264.

in [1] and we showed how to construct rotation Gaussian–Hermite invariants even in the cases when no explicit invariants from geometric moments are available. We theoretically proved the independence and completeness of the new invariants and showed that object symmetry makes certain invariants zero. Since we work in centralized coordinates, all invariants are automatically invariant also to the image translation.

We proved experimentally that the maximum achievable order of Gaussian–Hermite moments is much higher than that of geometric moments and, at the same time, GHMs are calculated with a better precision than GMs, which makes GHMs powerful and discriminative features for object description. This is the main achievement of the paper.

Another remarkable advantage of Gaussian–Hermite moments is that their area of orthogonality is the whole plane. This property differentiates the GHMs from most of the orthogonal moments which are commonly used in image analysis, such as Legendre, Zernike, and Chebyshev moments [2]. These moments are orthogonal on a bounded region (square or circle). To calculate them on an image, we would have to map the whole image into the area of orthogonality. Even if this mapping is performed correctly, it may introduce some errors into the moment calculation, particularly when we have to map the image into a circle. If the mapping is incorrect and certain part of the image lies outside the area of orthogonality (for instance due to the spatial transformation of the image), the moment calculation fails completely. In the case of the GHMs, no mapping is necessary and there is no danger of a precision loss of this kind.

Extension of the invariance property also to scaling is, however, more complicated than in the case of geometric moments. Due to the parameter $\sigma$, we cannot normalize the GHMs to scaling but we have to perform a full search in the scale space.

## Acknowledgements

This work has been partially supported by the Czech Science Foundation under the Grant no. GA15-16928S. A part of this work was done when B. Yang was a postdoc at the Institute of Information Theory and Automation of the CAS.

## References

[1] B. Yang, M. Dai, Image analysis by Gaussian-Hermite moments, Signal Process. 91 (2011) 2290–2303.
[2] J. Flusser, T. Suk, B. Zitová, Moments and Moment Invariants in Pattern Recognition, Wiley, Chichester, 2009.
[3] J. Flusser, On the independence of rotation moment invariants, Pattern Recognit. 33 (9) (2000) 1405–1410.
[4] M.R. Teague, Image analysis via the general theory of moments, J. Opt. Soc. Am. 70 (8) (1980) 920–930.
[5] A. Khotanzad, Y.H. Hong, Invariant image recognition by Zernike moments, IEEE Trans. Pattern Anal. Mach. Intell. 12 (5) (1990) 489–497.
[6] Å. Wallin, O. Kübler, Complete sets of complex Zernike moment invariants and the role of the pseudoinvariants, IEEE Trans. Pattern Anal. Mach. Intell. 17 (11) (1995) 1106–1110.
[7] K.M. Hosny, New set of rotationally Legendre moment invariants, Int. J. Electr. Electron. Eng. 4 (2010) 176–180.
[8] P.-T. Yap, R. Paramesran, S.-H. Ong, Image analysis by Krawtchouk moments, IEEE Trans. Image Process. 12 (11) (2003) 1367–1377.
[9] Y.J. Li, Reforming the theory of invariant moments for pattern recognition, Pattern Recognit. 25 (1992) 723–730.
[10] B. Yang, G.X. Li, H.L. Zhang, M. Dai, Rotation and translation invariants of Gaussian–Hermite moments, Pattern Recognit. Lett. 32 (2011) 1283–1298.